ASM | Applied and Environmental Microbiology

| Bacteriology | Full-Length Text

Aromatic lactic acid production by *Bifidobacterium longum* subsp. *infantis* is determined by cell density, substrate availability, and pH *in vitro*

Thilde Garbøl Plenge,[1] Mikael Pedersen,[1] Martin Frederik Laursen[1]

AUTHOR AFFILIATION See affiliation list on p. 14.

ABSTRACT *Bifidobacterium longum* subsp. *infantis (B. infantis*) is an important colonizer of the infant gut. This species is known to produce a variety of health-beneficial metabolites, including aromatic lactic acids (ALAs), supporting early-life immune development. However, the regulation of ALA production in *B. infantis* remains poorly understood. In this study, we investigated how environmental factors, such as substrate availability and pH, affect *B. infantis* DSM20088 growth and ALA production *in vitro*. Bacterial batch cultivations supplemented with different amino acid concentrations revealed a linear relationship between indole-3-lactic acid (ILA), 4-hydroxyphenyllactic acid (OH-PLA), and phenyllactic acid (PLA) production, and exogenous concentrations of tryptophan, tyrosine, and phenylalanine, respectively. Furthermore, chemostat cultivations at physiologically relevant pH levels (4.5, 5.5, and 6.5) showed that an acidic pH slowed growth and shifted ALA production by *B. infantis*. Overall, ALA concentrations correlated strongly with bacterial abundance across and within pH levels, showing that cell density is a major determinant of ALA production. After considering the growth-limiting effects of lower environmental pH, it had a limited impact on the total production of ALAs, but the relative production of PLA was stepwise enhanced at more acidic pH at the expense of ILA, independent of cell density. In conclusion, this study shows that cell density, substrate availability, and environmental pH determine aromatic lactic acid production by *B. infantis*.

IMPORTANCE *Bifidobacterium longum* subsp. *infantis* can be an abundant bacterial species in the infant gut microbiota, where it supports immune development, e.g., through the production of aromatic lactic acids. In this study, we cultured *Bifidobacterium longum* subsp. *infantis* at different concentrations of aromatic amino acids and pH levels to investigate the effect of these environmental factors on aromatic lactic acid production. We show that there is a linear relationship between aromatic lactic acid production and the exogenous aromatic amino acid concentration, that the production strongly follows cell density, and that pH regulates the preference toward producing different aromatic lactic acids. This knowledge may help inform strategies to enhance or direct beneficial aromatic lactic acid (ALA) production in the infant gut.

KEYWORDS chemostat, substrate availability, phenyllactic acid, indole-3-lactic acid, 4-hydroxyphenyllactic acid, *Bifidobacterium longum* subspecies *infantis*, metabolites, *in vitro*, infant gut, pH

"Infant-type" *Bifidobacterium* species, such as *B. longum, B. bifidum,* and *B. breve*, are important members of the early life gut microbiota. These species are promoted by breastfeeding due to their ability to metabolize human milk oligosaccharides (HMOs), the third-most abundant solid component in breastmilk (1). *Bifidobacterium longum*

Editor Knut Rudi, Norwegian University of Life Sciences, Ås, Norway

Address correspondence to Martin Frederik Laursen, mfrla@food.dtu.dk.

The authors declare no conflict of interest.

See the funding table on p. 14.

Received 17 December 2025
Accepted 13 April 2026
Published 6 May 2026

subsp. *infantis* (*B. infantis*) in particular has a prodigious capacity to grow on HMOs (2) and dominate the gut ecosystem in breastfed infants (3). Moreover, high abundance of *B. infantis* contributes to beneficial immune maturation, reduced intestinal inflammation, and improved intestinal barrier integrity (4).

One way by which *B. infantis* contributes to host physiology is through the production of metabolites, including aromatic lactic acids (ALAs) (5). ALAs are derived from the aromatic amino acids (AAAs), tryptophan, tyrosine, and phenylalanine, which are metabolized to indole-3-lactic acid (ILA), phenyllactic acid (PLA), and 4-hydroxyphenyllactic acid (OH-PLA), respectively. It has been shown that ALAs aid in immune regulation by serving as ligands for host cell receptors. Especially, ILA is recognized for its ability to activate the aryl hydrocarbon receptor, which is involved in epithelial barrier function, protection against pathogens, and regulation of host metabolism (6, 7). Additionally, ILA and PLA are potent ligands for the hydroxycarboxylic acid receptor 3 (HCA_3), a regulator of immune functions and energy homeostasis (5, 8, 9). ALAs also serve as antimicrobial agents (10–12) and have been suggested to reduce the prevalence of *Escherichia coli* and other antimicrobial resistance gene-rich taxa in the infant gut (13). Last, fecal levels of OH-PLA at 2 months of age were recently shown to associate inversely with later risk of IgE-mediated allergic sensitization in the Swedish ALADDIN cohort and decrease IgE production *ex vivo* (14).

B. infantis produces ALAs via a catabolic pathway that likely begins with the transamination of AAAs into aromatic pyruvic acids, which are subsequently converted to ALAs by the aromatic lactate dehydrogenase Aldh (5). While it has been shown that "infant-type" *Bifidobacterium* species, including *B. infantis,* produce ALAs in the infant gut (5), how the gut environment affects the accumulation of these metabolites remains unknown.

Physical and chemical factors in the intestinal environment, such as nutrient availability, pH, and transit time, all influence the composition and metabolic activity of the microbiota (15, 16). Infants are usually fed breastmilk, formula, or a combination of both, each providing different substrates available for bacterial fermentation in the gut. Although commercial formula is designed to mimic human milk, most formulas contain no or limited amounts/types of HMOs, leading to a lower abundance of "infant-type" *Bifidobacterium* species (17). Additionally, the AAA content in human milk changes during the lactation period and differs between formula brands (18). Since AAA concentrations direct ALA production by lactic acid bacteria (19), amino acid availability might play a role in ALA production by *B. infantis*. Moreover, correlations between the abundance of "infant-type" *Bifidobacterium* species and ALA concentrations in infant feces have been observed (5), suggesting that higher cell densities of producer species result in higher production of ALAs. However, since a high abundance of *Bifidobacterium* species, in particular *B. infantis*, is also negatively correlated to fecal pH (20), a lower gastrointestinal pH, favoring ALA production, might also explain the higher concentrations of ALAs. Supporting this, it has been reported that acid stress leads to upregulation of genes involved in amino acid metabolism in *B. longum* subsp. *longum* (21), highlighting the possibility that pH regulates ALA production. We therefore investigated how AAA substrate availability, cell density, and environmental pH affect ALA production by *B. infantis* DSM20088.

RESULTS

ALA production follows AAA availability in a dose-dependent manner

To test the effect of amino acid availability on ALA production, batch cultures of *B. infantis* were grown in MRS-cys broth supplemented with different concentrations of AAAs. After 48 h of growth, optical density (OD_{600nm}) and metabolite accumulation were assessed. All cultures reached an OD_{600nm} between 2.6 and 3.6 (Fig. S1A). The cultures with the highest amino acid supplementation (0.2%) grew to a slightly, but significantly lower OD_{600nm} than non-supplemented cultures, indicating that the starting concentration of AAAs or accumulating metabolites slightly limits final cell densities under these

conditions. ILA, OH-PLA, and PLA were not detected in the MRS-cys broth control. In inoculated cultures, explicit production of these metabolites was observed (Fig. 1A). PLA was the most abundant ALA in the non-supplemented culture (208 ± 29 µM), followed by OH-PLA (105 ± 13 µM) and ILA (50 ± 8 µM). This is in line with phenylalanine being a major aromatic amino acid in MRS-cys broth (Fig. S1B) and has been reported previously (5).

In tryptophan, tyrosine, and phenylalanine supplemented cultures, a significant increase in ILA, OH-PLA, and PLA was observed, respectively (Fig. 1A). Moreover, the production of each ALA showed a strong linear relationship with the percent of supplemented AAA (Fig. 1B). ILA and PLA showed clear proportional relationships and very strong positive correlations with the detected tryptophan and phenylalanine concentrations, respectively (Fig. S1C). OH-PLA did not correlate with measured tyrosine concentrations, but this result is suspected to be caused by technical issues of tyrosine quantification.

ALA production is tightly coupled to cell density

To investigate the effect of different physiological pH levels on ALA production, *B. infantis* was cultivated in chemostat cultures maintained at constant pH levels of 4.5, 5.5, and 6.5 (Fig. 2A). The cultures were grown for 24 h in batch mode and thereafter in chemostat mode until 96 h (Fig. 2B). For pH 6.5 and 5.5 cultures, there was no significant difference in OD_{600nm} over time (Fig. S2A). Additionally, these cultures grew with similar growth

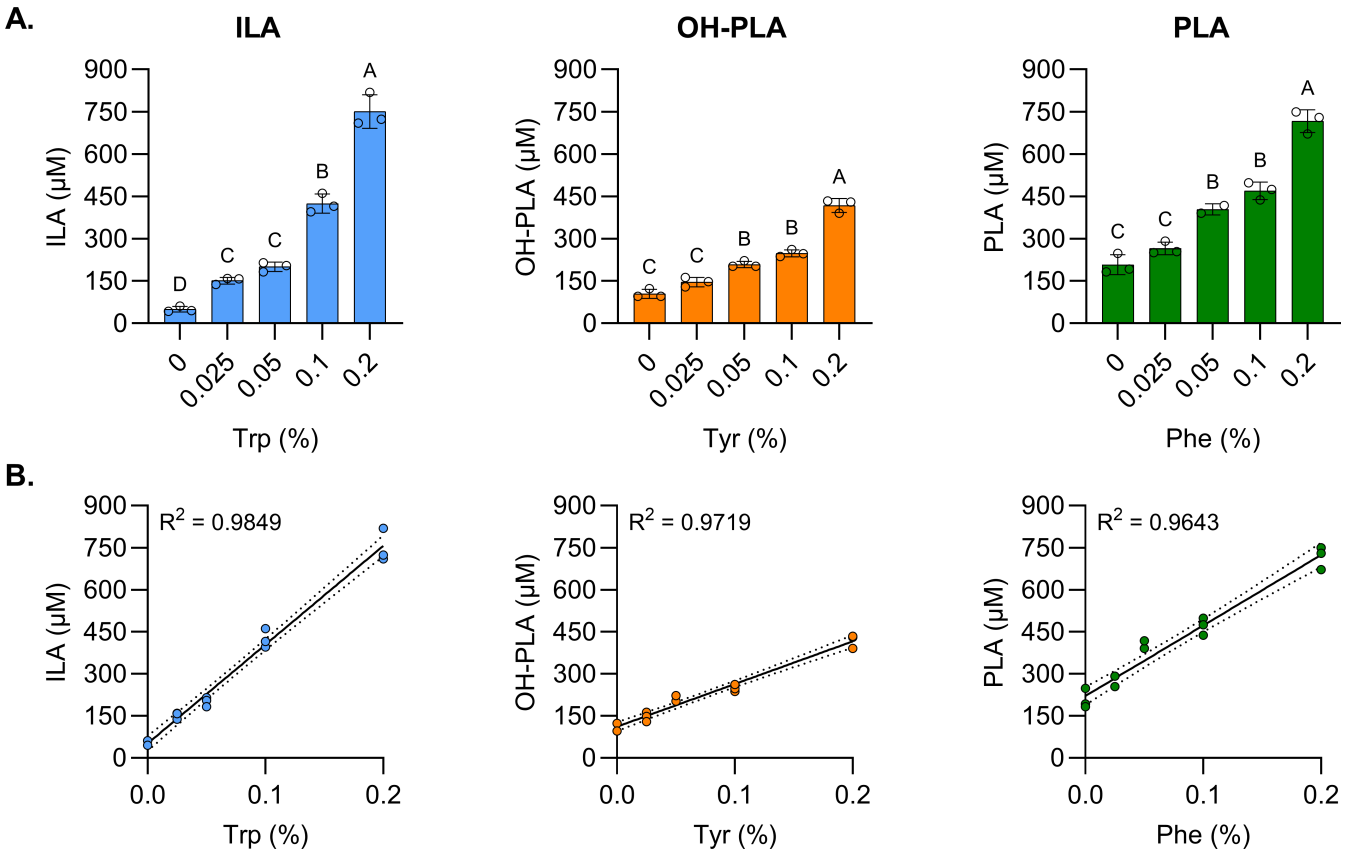

FIG 1 Aromatic lactic acid concentrations (µM) in *B. infantis* batch cultures grown for 48 h in MRS-cys medium with aromatic amino acid supplementation. (A) Increase in aromatic lactic acid concentration in response to supplementation. Bars show mean ± s.d. of three biological replicates. Statistical significance was evaluated by one-way analysis of variance (ANOVA), followed by Tukey's multiple comparisons test. Means not sharing letters are significantly different with adjusted $P < 0.05$. (B) Linear relationship between aromatic lactic acid concentration and percent supplemented aromatic amino acid, with R^2-values shown in the figure. Points ($n = 15$) show a single biological replicate. ILA, indole-3-lactic acid; PLA, phenyllactic acid; OH-PLA, 4-hydroxyphenyllactic acid; Trp, tryptophan; Phe, phenylalanine; Tyr, tyrosine.

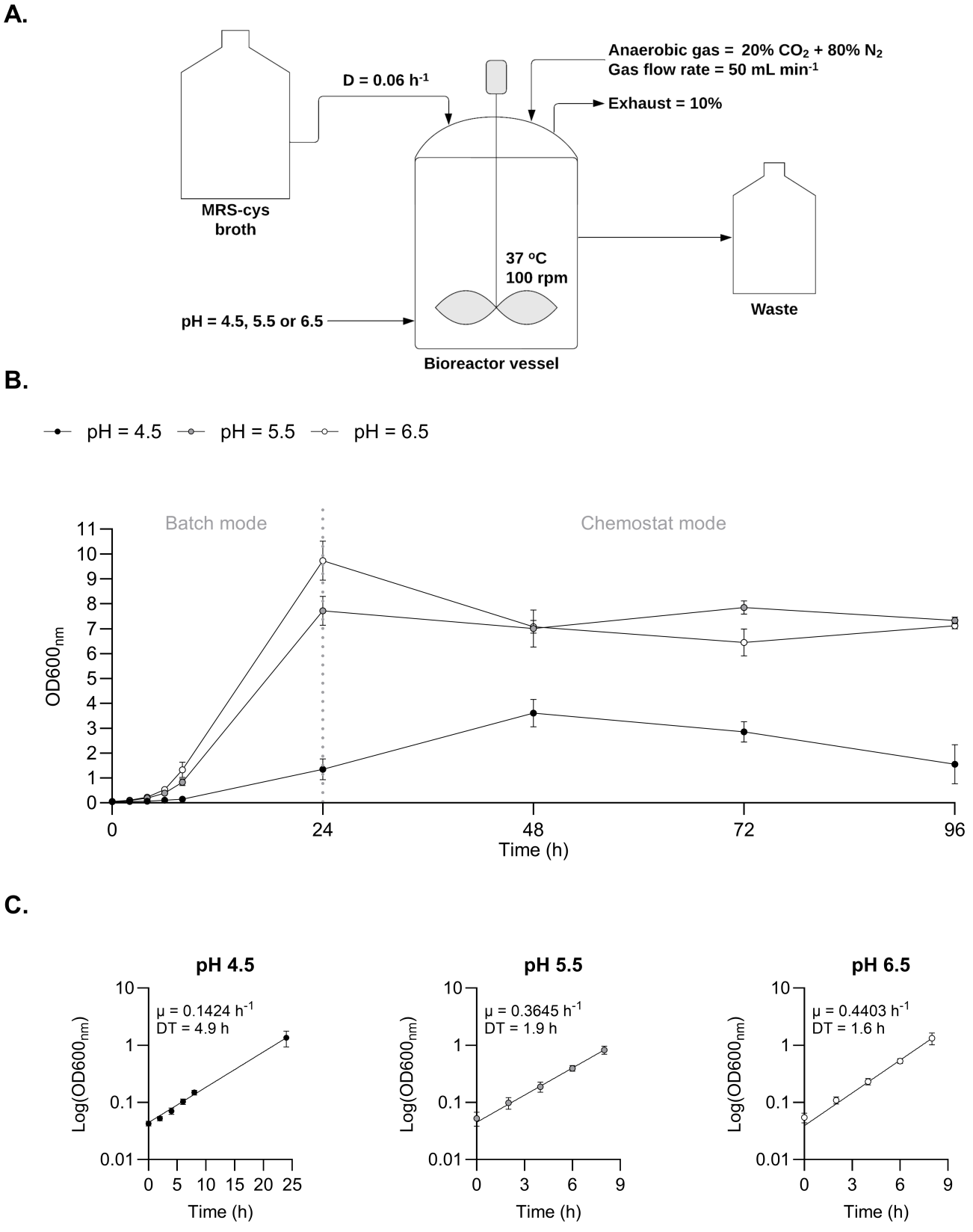

FIG 2 Chemostat cultures of *B. infantis* at different pH levels. (A) Chemostat culture parameters. (B) Optical densities (OD_{600nm}) over time. The cultures were run in batch mode for the first 24 h, whereafter chemostat mode was applied. Points show mean ± s.d. of three biological replicates. (C) Log-transformed optical densities (OD_{600nm}) of *B. infantis* during the exponential growth phase, with the specific growth rate (μ) and doubling time (DT) at each pH level. Points show mean ± s.d. of three biological replicates.

rates (Fig. 2C). pH 5.5 cultures maintained a constant OD_{600nm} from 24 h onward, while pH 6.5 cultures' OD_{600nm} stabilized after 48 h (Fig. 2B). Growth was to some extent inhibited at pH 4.5 since both the growth rate (Fig. 2C) and OD_{600nm} over time (Fig. S2A) were significantly lower than for the less acidic pH conditions. pH 4.5 cultures did not show a stabilization in OD_{600nm} when applying chemostat mode (Fig. 2B). For the first 24 h of chemostat mode, the pH 4.5 culture continued to increase and peaked at the 48-h time point. Hereafter, a decrease in OD_{600nm} was observed. Consistently, colony-forming unit (CFU) counting over time showed a significant decrease in viable cell numbers only at pH 4.5 between 48 and 96 h, whereas cell numbers were kept stable around $\approx 10^9$ CFU mL^{-1} for pH 5.5 and 6.5 between 48 and 96 h (Fig. S2B). As expected, CFU counts over time were strongly and significantly correlated with OD_{600nm}, supporting the growth patterns of *B. infantis* observed in OD_{600nm} measurements across the different pH conditions (Fig. S2C).

Total and individual ALA concentrations largely followed OD_{600nm} measurements over time within each pH condition (Fig. 3A). In general, higher ALA concentrations were observed for pH 5.5 and 6.5 compared to pH 4.5 (Fig. S3), mirroring the growth differences. Across pH conditions, ALA concentrations correlated positively with OD_{600nm} (Fig. 3B) and CFU mL^{-1} of *B. infantis* (Fig. S4). At the individual pH levels, pH 4.5 and 6.5 also showed significant positive correlations between OD_{600nm} and ALAs (Fig. S5). This was not observed in pH 5.5 cultures, possibly explained by the steady state in cell density already after 24 h. Overall, this shows that the production of ALAs is tightly coupled to the cell density of *B. infantis*.

pH has limited influence on total ALA production but regulates preference toward the type of ALA produced

While ILA, OH-PLA, and total ALA concentrations were lower at pH 4.5 compared to both pH 5.5 and 6.5, PLA production did not differ between pH 4.5 and 6.5 (Fig. 3A; Fig. S3). However, PLA levels were lower at both pH 4.5 and 6.5 relative to pH 5.5. Additionally, OH-PLA concentrations were highest at pH 5.5, while ILA levels were highest at pH 6.5, significantly different from both other pH conditions. No significant difference in total ALA concentrations was observed between pH 5.5 and 6.5. However, since cell density had a pronounced impact on ALA production and varied across different pH levels, ALA concentrations were normalized to OD_{600nm}. Normalized concentrations showed a significant, but minor influence of pH on ALA production (Fig. 4). ILA exhibited the highest normalized production at pH 6.5, though this increase was only statistically significant relative to pH 5.5. The OD_{600nm} normalized OH-PLA levels were elevated at pH 4.5 compared to pH 6.5. Additionally, normalized PLA concentrations were higher at both pH 4.5 and 5.5 compared to pH 6.5. The total OD_{600nm} normalized production of ALAs was significantly higher at pH 4.5 than at the other tested pH conditions, mostly driven by the elevated PLA production. However, since there were no differences in normalized total ALA production between pH 5.5 and 6.5, and a limited difference to pH 4.5 (somewhat driven by the decrease in cell density over time under this condition), it appears that pH regulates the preference toward producing different ALAs rather than the total production. To investigate this further, the relative percentwise abundance of the three ALAs at the different time points was compared (Fig. 5). At pH 6.5, an almost equal abundance of the three ALAs was observed. Oppositely, when lowering the pH, a stepwise shift toward higher PLA and less ILA production occurred. Therefore, taking into account its effect on growth, environmental pH has limited influence on the total production of ALAs but rather seems to regulate the preference toward the type of ALA produced.

Acidic pH conditions lead to subtle upregulation of *aldh* expression and affect several *aat* genes

The *aldh* gene is responsible for the last step in the formation of ALAs by "infant"-type *Bifidobacterium* species (5). To get a deeper understanding of pH-regulated

ALA production, we therefore quantified *aldh* (BLON_RS05510) expression by reverse transcription quantitative polymerase chain reaction (RT-qPCR). It was indicated that an

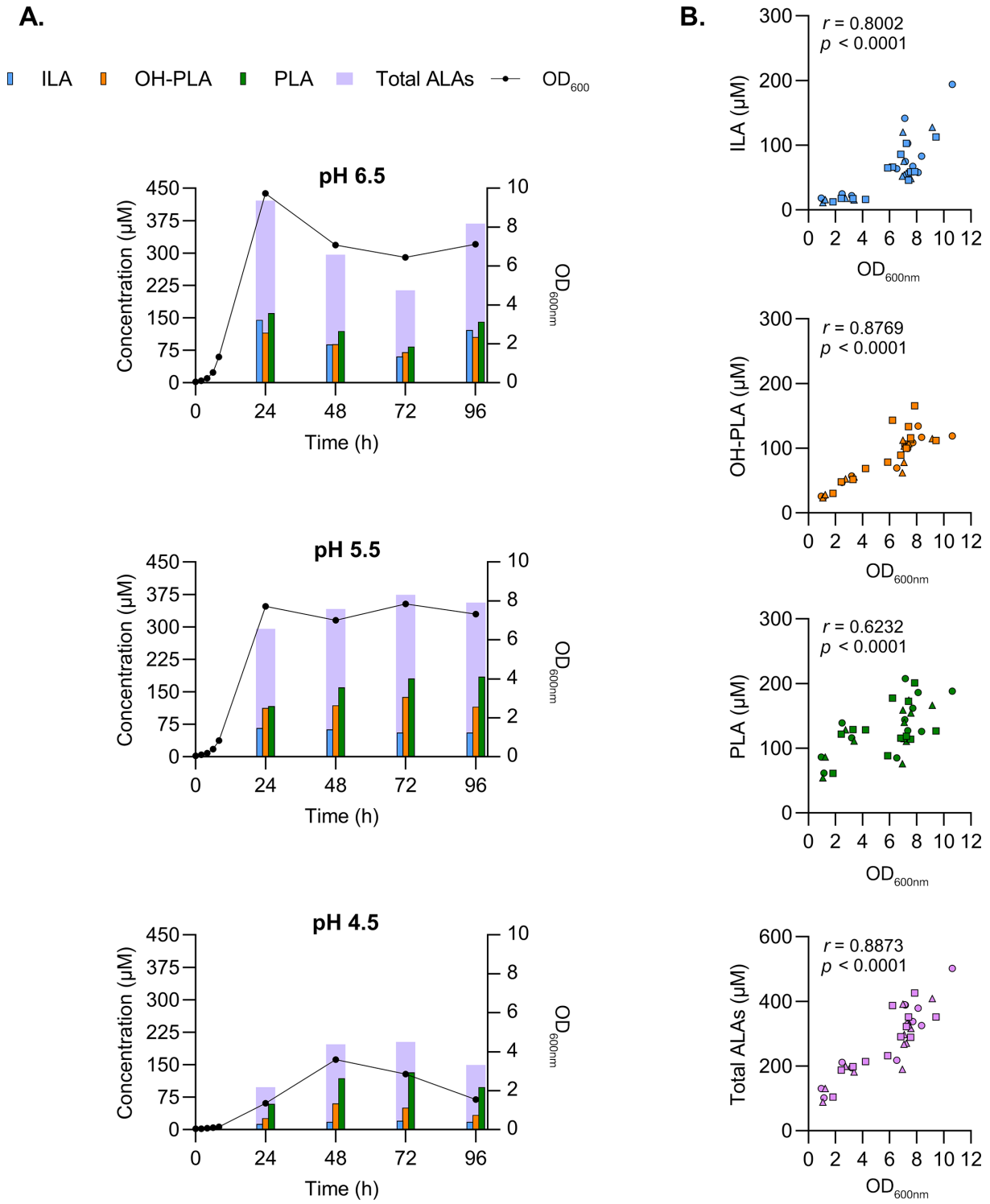

FIG 3 Aromatic lactic acid production and growth of *B. infantis* in chemostat cultures at different pH levels. (A) ILA, OH-PLA, PLA, total ALA concentrations (μM), and optical densities (OD_{600nm}) over time. Bars and points show means of three biological replicates. (B) Correlations (n = 36) between optical density (OD_{600nm}) and ALAs (μM) in chemostat cultures at 24–96 h, with Pearson correlation coefficients (r) and *P* values (two-tailed) shown in the figures. Biological replicates across pH levels are shown as triangles, squares, and circles. ILA, indole-3-lactic acid; PLA, phenyllactic acid; OH-PLA, 4-hydroxyphenyllactic acid; ALAs, aromatic lactic acids.

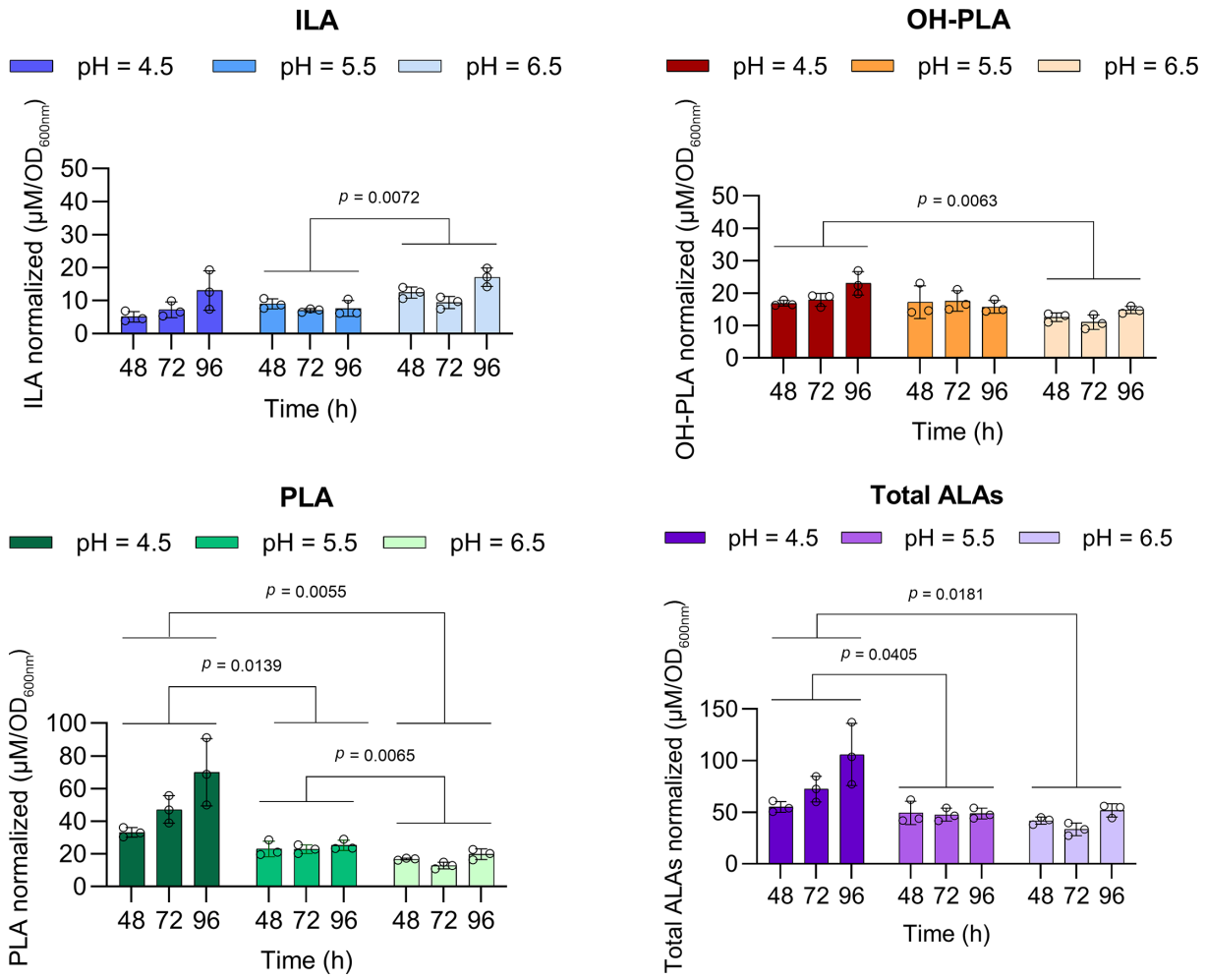

FIG 4 Normalized aromatic lactic acid production by *B. infantis* grown in chemostat cultures at different pH levels during steady state. Aromatic lactic acid concentrations normalized with OD_{600nm} (μM/OD_{600}) at different pH levels. Bars show mean ± s.d. of three biological replicates. Statistical significance between groups was evaluated with two-way ANOVA, with *P* values of the pH effect shown on the figures. ILA, indole-3-lactic acid; PLA, phenyllactic acid; OH-PLA, 4-hydroxyphenyllactic acid; ALAs, aromatic lactic acids.

acidic pH leads to a slight upregulation of *aldh* (Fig. 6A), consistent with the slightly higher normalized ALA concentration at pH 4.5 (Fig. 4). However, since the major effect of pH was a shift in the type of ALA being produced, we hypothesized that other genes involved in the initial step of aromatic amino acid metabolism might exhibit more dramatic pH-driven changes. Therefore, RNA sequencing (RNA-seq) was conducted to assess global transcription. Overall, RNA-seq analysis mainly revealed upregulation of several genes associated with general acid stress at pH 4.5 (Table S4). Genes of the *atp* operon encoding the F_1F_0-ATPase were consistently upregulated compared to pH 5.5 and 6.5, in line with the proposed role of F_1F_0-ATPase in maintaining intracellular pH through proton extrusion in *Bifidobacterium* (22). Furthermore, type I glutamate-ammonia ligase and ketol-acid reductoisomerase genes, suggested to contribute to intracellular pH buffering, as well as molecular chaperones involved in protein quality control (*dnaK*, *groEL*, *groES*) (22), were also induced at pH 4.5.

In agreement with the RT-qPCR, RNA-seq also showed a slight upregulation of the *aldh* gene, especially at pH 4.5 (Fig. 6B). Because *aldh* is located within a genetic element that contains a haloacid dehalogenase gene (*had*) (BLON_RS05515) and an amino-acid transaminase gene (*aat*) (BLON_RS05520), we examined the expression patterns of these neighboring genes as well (Table 1). The *had* gene followed the expression pattern of

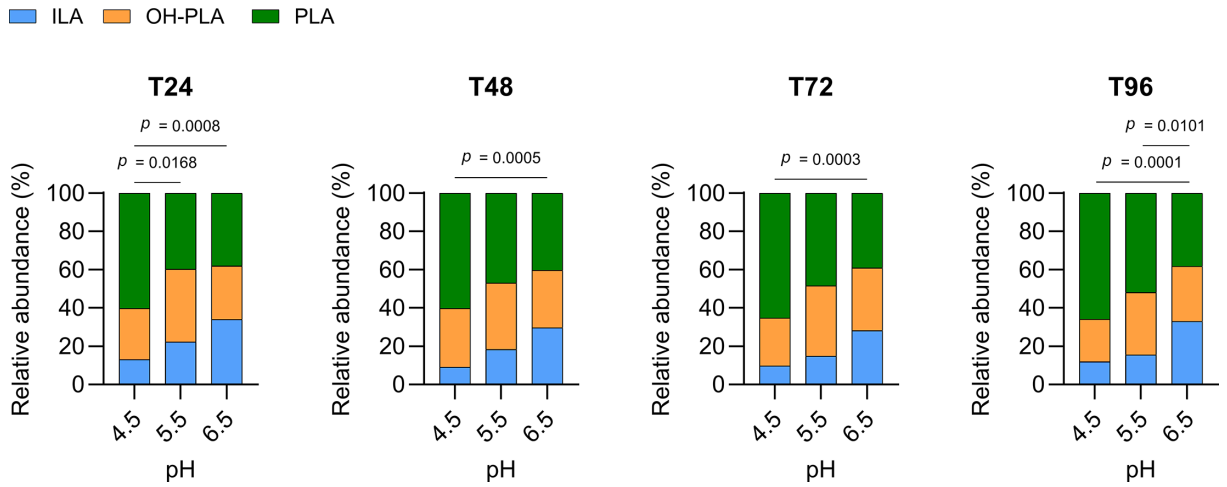

FIG 5 Preference in aromatic lactic acid production by *B. infantis* grown in chemostat cultures at different pH levels. Relative distributions (%) of aromatic lactic acids at different time points. Stacked bars show the means of three biological replicates. Statistical significance was assessed using the chi-square test with *P* values displayed in the figure panels. ILA, indole-3-lactic acid; PLA, phenyllactic acid; OH-PLA, 4-hydroxyphenyllactic acid; ALAs, aromatic lactic acids.

aldh and showed a small upregulation at pH 4.5 and 5.5 compared to pH 6.5. Interestingly, the *aat* gene was, on the other hand, consistently more than twofold upregulated at pH 4.5 compared to the less acidic conditions, with no differential expression observed between pH 5.5 and 6.5. In *B. breve*, a different *aat* gene has been shown to play a key role in ALA production (23). The *B. infantis* homolog (BLON_RS07465) did not show a consistent change in expression when comparing the different pH conditions (Table 1). Overall, several genes annotated as aminotransferases were either up- or downregulated in response to low pH (Table 1), suggesting that the cells are actively rebalancing amino acid metabolism in response to acid stress. Overall, these results suggest that pH-mediated differential regulation of aminotransferases may explain the observed shifts in ALAs produced across pH conditions.

DISCUSSION

"Infant-type" *Bifidobacterium* species, including *B. infantis*, are key producers of immune-regulating ALAs in the infant gut (5). However, the factors that determine ALA abundance remain poorly understood. To address this gap, we investigated how environmental factors affect ALA production by *B. infantis in vitro*.

First, we showed that ALA production follows the availability of exogenous AAAs, suggesting that higher dietary AAA levels may lead to increased ALA levels in the infant gut. This observation is consistent with patterns reported in lactic acid bacteria (LAB), where PLA and OH-PLA production increase in response to phenylalanine and tyrosine supplementation (19, 24), and with the dose-dependent relationship between tryptophan and ILA described for *Clostridiales* species (25). However, as MRS is a complex medium containing peptides, free amino acids, and other growth factors, interactions with these components may influence AAA uptake and metabolism. Consequently, our study demonstrates a dose-dependent linear relationship between AAA availability and ALA production, but a more precise quantitative dose–response relationship for *B. infantis* would require the use of a chemically defined medium in future studies. Additionally, it remains to be established if AAA diet supplementation in early life will, in fact, increase gastrointestinal and circulating ALA levels. We have previously demonstrated that diet supplementation with tryptophan increases serum ILA concentration in gnotobiotic mice colonized with the ILA producer *Clostridium sporogenes* (25), indicating that substrate concentration-dependent production of ALAs also applies for *in vivo* settings. However, infant intervention studies using defined AAA diet supplementation regimes are required to elucidate this.

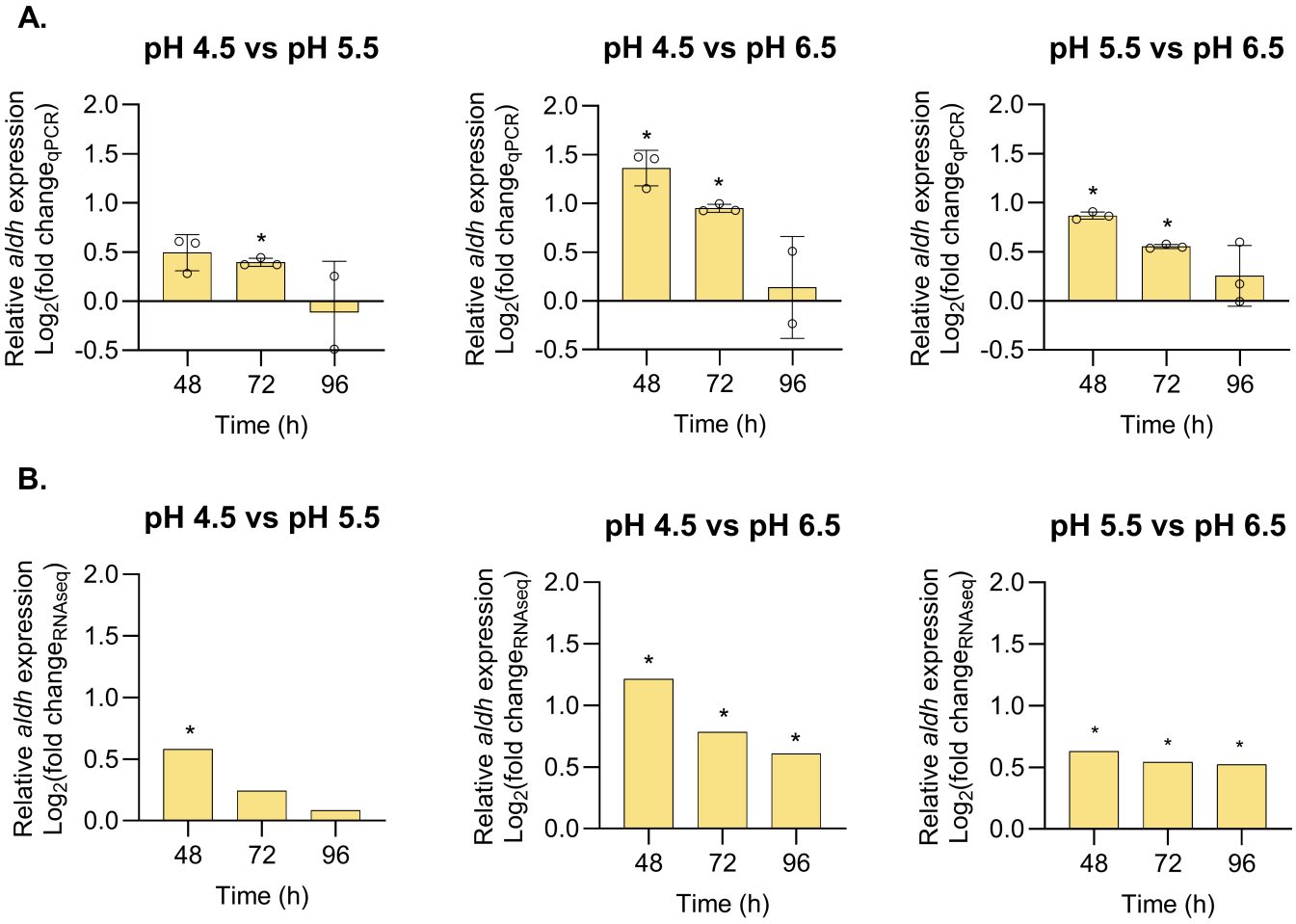

FIG 6 Relative aldh (BLON_RS05510) expression between pH conditions. (A) Log_2 fold change of the relative expression determined by RT-qPCR. Bars show mean ± s.d. of three biological replicates. Statistical significance was assessed using an unpaired two-tailed *t*-test with Welch's correction on gene expression values normalized to reference genes. *$P < 0.05$. (B) Log_2 fold changes at each time point, calculated from three biological replicates. *: Genes with an average read count greater than 100 across all samples and a false discovery rate (FDR)-corrected *P* value < 0.1 for the log_2 fold change are considered significant.

Next, we found that ALA production is tightly coupled to *B. infantis* cell density, indicating that bacterial abundance plays a crucial role in determining metabolite levels. This observation is consistent with reports of growth-associated ALA production in *Lactobacillus* (26, 27) and aligns with findings from Danish and Swedish infant cohorts, where fecal ALA concentrations positively correlated with the abundance of *B. longum* subsp. *infantis* (5, 14). Promoting growth of *B. infantis* may therefore be a strategy to enhance ALA production in the infant gut. Reciprocally, it has been suggested that ALA production promotes bacterial growth under nutrient-limited conditions. This has been shown *in vitro* for *B. breve,* where supplementing tryptophan and phenylalanine in an otherwise amino acid-limited defined medium had a strong positive effect on growth. Furthermore, mutants in the *aldh* gene did not exhibit the same fitness benefits as wild-type *B. breve*, indicating that ALA production is essential for growth under such conditions (23). However, conditions in the infant gut are unlikely to be amino acid-limited, and fecal AAA concentrations commonly exceed fecal ALA concentrations (28).

Since a high abundance of *B. infantis* is also linked to a low fecal pH (20), we next investigated how pH affects ALA production. We showed that growth is significantly inhibited at pH 4.5 compared to less acidic conditions (pH 5.5 and 6.5), consistent with the weak acid tolerance previously reported for *B. longum* (29). Furthermore, a pH of 4.5 led to upregulation of several acid stress response genes in *B. infantis*

TABLE 1 Differential expression of the had gene and genes encoding aminotransferases[a]

		pH 4.5 vs 5.5			pH 4.5 vs 6.5			pH 5.5 vs 6.5		
Gene name	**Gene ID**	**48 h**	**72 h**	**96 h**	**48 h**	**72 h**	**96 h**	**48 h**	**72 h**	**96 h**
HAD family hydrolase	BLON_RS05515	0.55*	0.19	−0.07	1.42*	1.00*	0.70*	0.87*	0.81*	0.77*
Aminotransferase class I/II-fold PLP-dependent enzyme	BLON_RS05520	1.80*	1.27*	0.99*	1.90*	1.28*	1.39*	0.10	0.01	0.40
PLP-dependent aminotransferase	BLON_RS03070	0.63*	0.45*	0.31	1.82*	1.88*	1.98*	1.20*	1.42*	1.66*
	BLON_RS07465	0.31	0.68*	0.47	0.46	0.85*	1.31*	0.15	0.17	0.83*
	BLON_RS10070	−1.11	−1.25*	−0.56	−1.43*	−1.51*	−1.87*	−0.32	−0.26	−1.31*
	BLON_RS11905	0.51	0.73*	0.57	0.95*	1.23*	2.02*	0.43	0.50	1.44*
	BLON_RS13315	0.72	−0.12	−0.38	0.34	−0.43	−4.37*	−0.38	−0.31	−4.00*
Aminotransferase class V-fold PLP-dependent enzyme	BLON_RS07165	−1.78*	−1.81*	−1.81*	−3.13*	−3.02*	−3.91*	−1.35	−1.21	−2.10*
Branched-chain amino acid aminotransferase	BLON_RS08165	1.07*	0.99*	0.76*	2.11*	1.79*	1.88*	1.05*	0.80*	1.12*
Phosphoserine transaminase	BLON_RS11090	1.38*	1.65*	1.46*	1.39*	1.69*	1.55*	0.01	0.03	0.08

[a]The table shows $\log_2$ fold changes at each time point, calculated from three biological replicates. *: Genes with an average read count greater than 100 across all samples and an FDR-corrected *P* value < 0.1 for the $\log_2$ fold change are considered significant.

(Table S4). This suggests that an acidic gut environment may slow bacterial growth and change metabolic fluxes, which in turn, both may affect overall ALA levels. In addition, the acid–base properties of ALAs may further influence bacterial physiology under acidic conditions. ALAs contain a carboxylic acid group and have pKa values in the range of ~3.6–4.1. Consequently, their protonation state depends on environmental pH according to the Henderson–Hasselbalch relationship. At lower pH conditions, a larger fraction of these metabolites exists in the undissociated form, which is more membrane-permeable and may diffuse back into the bacterial cells (22). Once inside the cytoplasm, dissociation of the acid can contribute to intracellular acidification and metabolic stress. Therefore, under highly acidic conditions, ALAs may not only represent excreted metabolic end products but could also act as weak acid stressors that potentially exacerbate growth inhibition. While we did not directly assess this mechanism, it may have contributed to the reduced growth and lower ALA accumulation observed at pH 4.5. Nonetheless, low fecal pH of 4.5–5.0 has been observed in breastfed infants, with gut microbiomes being highly dominated by *B. infantis* (30), indicating that some environmental conditions in the gut reduce its acid sensitivity.

Beyond the growth-mediated effects, pH had a distinct influence on ALA production by altering the ALA profile, favoring PLA production at the expense of ILA at lower pH. This is in line with acid stress triggering transcriptional and proteomic changes in amino acid metabolism in *B. longum* (21, 29). Since transamination has been described as the rate-limiting step for ALA synthesis in LAB (26, 31), and we observed differential expression of several *aat* genes in response to pH, we speculate that changes in aminotransferase activity may explain this shift in ALA profiles. Supporting this hypothesis, enhancing transamination by increasing the availability of the amino group acceptor α-ketoglutarate has been shown to increase ALA production by *B. infantis*, with PLA exhibiting the most pronounced increase (32). Furthermore, disruption of the transaminase AraT in *B. breve* severely impairs ILA production while having only minor effects on PLA and increasing 4-OH-PLA levels (23). Since AraT is required for the biosynthesis of phenylalanine and tyrosine, this suggests that other transaminases or anabolic pathways compensate by supplying pyruvic acid derivatives for these two amino acids in *B. breve* (23). To our knowledge, the exact aminotransferase(s) responsible for ALA production by *B. infantis* has not yet been identified, but it can be hypothesized that different routes for aromatic pyruvic acid production exist in *B. infantis* and that these are affected by pH.

Overall, our study shows that ALA production by *B. infantis* is regulated by environmental factors. We propose that ALA production can be enhanced through increased

AAA availability and *B. infantis* abundance, and that variations in pH may shape the composition of ALAs produced in the gut of infants.

MATERIALS AND METHODS

Bacterial strain and culture conditions

In this study, *Bifidobacterium longum* subsp. *infantis* DSM20088 (*B. infantis*) obtained from DSM (Deutsche Sammlung von Mikroorganismen, Germany) was used. The strain was stored in glycerol stocks at −80°C until use. Glycerol stocks were streaked on deMan–Rogosa–Sharpe agar (SSI Diagnostica, Cat. No. 50123) supplemented with 0.05% (wt/vol) L-cysteine hydrochloride (Sigma, Cat. No. C7477) (MRS-cys agar plates) and incubated for 48 h at 37°C in an anaerobic chamber (Don Whitley Scientific Limited) containing 10% H_2, 10% CO_2, and 80% N_2 gases. For overnight cultures, single colonies were resuspended in MRS-cys broth (33) and incubated for 20–24 h at 37°C in the anaerobic chamber.

The MRS-cys broth contained 10 g/L Peptone from casein (Merck, Cat. No. 1.07213.1000); 8.0 g/L Meat extract (Oxoid, Cat. No. LP0029); 4.0 g Yeast extract (Oxoid, Cat. No. LP0021); 2.0 g/L Di-potassium hydrogen phosphate (Merck, Cat. No. 1.05104.1000); 5.0 g/L Sodium acetate (Sigma, Cat. No. S8750), 2.0 g/L Tri-ammonium citrate (Sigma, Cat. No. A1332); 0.2 g Magnesium sulfate heptahydrate (Merck, Cat. No. 1.05886.0500); 0.05 g/L Manganous sulfate monohydrate (Sigma, Cat. No. M7634) supplemented with sterile filtered 0.05% (wt/vol) L-cysteine hydrochloride (Sigma, Cat. No. C7477) and 2% (wt/vol) D-glucose (Merck, Cat. No. G8270) after autoclavation.

Batch fermentation with aromatic amino acid supplementation

To test how ALA production by *B. infantis* is affected by AAA availability, *in vitro* fermentations with different initial concentrations of AAAs were set up. Singles colonies of *B. infantis* were inoculated into MRS-cys broth supplemented with 0.025%, 0.05%, 0.1%, and 0.2% (wt/vol) sterile filtered L-tryptophan (Sigma, Cat. No. T0254), L-phenylalanine (Sigma, Cat. No. P2126), or L-tyrosine disodium salt dihydrate (Merck, Cat. No. 1.02413.0100) and incubated in the anaerobic chamber at 37°C. Each AAA-supplemented culture was evaluated in biological triplicate and MRS-cys broth without supplementation served as a control. After 48 h of growth, the optical density at 600 nm was measured in a 96-well plate using a PowerWave HT Microplate Spectrophotometer (BioTek). All cultures were centrifuged at 15,000 × *g* for 10 min at 4°C, and the supernatants were stored at −20°C until liquid chromatography-mass spectrometry (LC-MS) analysis.

Chemostat cultivations at different pH levels

To test the influence of pH on ALA production, *B. infantis* was grown in chemostat cultures at a dilution rate of 0.06 h^{-1} in a 1 L Biostat A bioreactor (Sartorius). The temperature was kept constant at 37°C, the pH was controlled at constant levels (4.5, 5.5, and 6.5) by automatic addition of 1 M HCl and 2 M NaOH, and the stirring speed was 100 rpm. To maintain anaerobic conditions, the headspace was flushed with 80% (vol/vol) N_2 and 20% (vol/vol) CO_2 gases at a rate of 50 mL min^{-1}. The chemostat cultures were prepared by adding 500 mL MRS broth to the bioreactors, followed by autoclavation of the entire setup. Subsequently, sterile filtered L-cysteine-HCl (0.5 g L^{-1}) and D-glucose (20 g L^{-1}) were added. After an overnight pre-run to ensure anaerobic conditions, the bioreactors were inoculated 1:100 with an overnight culture made in MRS-cys broth as previously described. After 24 h of growth (batch mode), in- and outflow was applied, and continuous fermentation (chemostat mode) was run for a further 72 h. Bacterial growth was monitored by measuring the optical density at 600 nm using a spectrophotometer. To determine the concentration of viable cells during the experiment, CFUs mL^{-1} were estimated. Samples were serially diluted in MRS-cys

broth, and appropriate dilutions were plated on MRS-cys agar plates in duplicates. The plates were incubated at 37°C in the anaerobic chamber for 48 h, after which CFUs were counted. For metabolite quantification, samples were centrifuged at 15,000 × *g* for 10 min at 4°C, and the supernatants were stored at −20°C until LC-MS analysis. For RNA analysis, one volume of sample was immediately mixed with two volumes of RNAProtect Bacteria Reagent (QIAGEN, Cat. No. 76506). The stabilized solution was pelleted according to the manufacturer's instructions and stored at −80°C until RNA extraction.

Identification and quantification of aromatic lactic acids by LC-MS

For quantification of ALAs and AAAs, LC-MS was performed. For the LC-MS, isotopic-labeled L-tryptophan (indole-d5, 98%) (Cambridge Isotope Laboratories) was used as an internal standard. To quantify the aromatic compounds, different concentrations of analytes (0, 0.8, 2, and 4 µg mL^{-1}) were prepared by mixing the analyte mix (Table S1), internal standard, and sterile water. Furthermore, quality control (QC) standards were prepared and processed in the same way as samples to normalize against any loss or gain of the analytes during data processing. The QC standards were prepared in triplicate of 80 µL by mixing growth media 1:1 with analyte mix (each analyte at 40 µg/mL).

To prepare samples for LC-MS, culture supernatants were thawed at 4°C and then centrifuged at 16,000 × *g* at 4°C for 10 min. A volume of 80 µL supernatant was transferred to a new tube. To each sample and QC standard, 20 µL internal standard (40 µg mL^{-1}) and 300 µL acetonitrile (Sigma, Cat. No. 1003363276) were added. The samples were vortexed for 10 s and placed at −20°C for 10 min to precipitate proteins. Afterward, the samples were centrifuged at 16,000 × *g* at 4°C for 10 min. A volume of 50 µL of supernatant of each sample, followed by 50 µL of sterile water, was transferred to a liquid chromatography vial (resulting in a 1:10 dilution of the sample and an internal standard concentration of 1 µg mL^{-1}).

The LC-MS was performed as previously described (5). In brief, samples (5 µL) were injected and analyzed by a UPLC-QTOF-MS system, utilizing a Dionex Ultimate 3000 RS liquid chromatograph coupled to a Bruker maXis time-of-flight mass spectrometer with an electrospray interphase (Bruker Daltonics). The analytes were separated on a Poroshell 120 SB-C18 column with a dimension of 2.1 × 100 mm and 2.7 µm particle size (Agilent, Cat. No. 685775-902). The LC-MS data from negative electrospray ionization mode were processed using QuantAnalysis v.2.2. Peak area ratios were calculated as the integrated area of the metabolite peak divided by the area of the internal standard peak. Standard curves were generated for each metabolite and used to determine its concentration in the samples.

ALAs were measured at the end of fermentation in batch cultures and from 24 h onward in chemostat cultures. In chemostat culture supernatants at pH 4.5, only PLA was measured above 0.8 µg mL^{-1}. However, since extracted chromatograms for both ILA and OH-PLA were identified as clear peaks, extrapolated data were used for quantification.

Transcriptome analysis

Gene expression in response to different pH levels was analyzed by RT-qPCR and RNAseq.

RNA from chemostat samples was extracted by using the RNeasy Mini kit (Qiagen, Cat. No. 74106) with minor modifications. In brief, 600 µL RLT lysis buffer was added to each sample, followed by 10 µL of β-mercaptoethanol to inactivate RNase activity. The samples were then transferred to bead columns and placed in a bead beater (Retch) for 30 s at 30 Hz to mechanically disrupt cells. After bead beating, the samples were centrifuged at 8,000 × *g*, and the supernatant was mixed 1:1 with 80% ethanol. Subsequent extraction steps were performed according to the RNeasy Mini Kit spin column purification protocol. The concentration of extracted RNA was determined using Qubit RNA high sensitivity assay (Invitrogen, Cat. No. Q32852), and the purity was assessed on the Nanodrop by measuring the A260/A280 and A260/A230 ratios. Samples

used for RNAseq included a DNase step (Qiagen, Cat. No. 79254) in the RNA extraction as described in the RNeasy Mini Kit spin column purification protocol.

For RT-qPCR, isolated RNA was reverse transcribed into cDNA using the reverse transcription protocol for SuperScript IV VILO Master Mix with ezDNase enzyme (Invitrogen, Cat. No. 11766050).

To normalize *aldh* gene expression, *pdxS* and *gluC* were used as reference genes (34). Primers were designed for *aldh* and reference genes using Primer3web v. 4.1.0 (https://primer3.ut.ee/), considering the following parameters: primer size (18–23 bp), CG% (30–70), primer melting temperature (Tm 55°C–65°C), and product size range (100–200 bp). The specificity of the primers was tested *in silico* using BLAST analysis against the genome of *Bifidobacterium longum* subsp. *infantis ATCC 15697 = JCM 1222 = DSM 20088 (NCBI:txid391904*). To determine primer efficiencies, qPCR reactions with 10-fold dilutions of genomic DNA extracted from an O/N culture of *B. infantis* using DNeasy UltraClean Microbial kit (Qiagen, Cat. No. 12224-50) were set up using the method described below. Acceptable primer pairs had PCR efficiencies between 90% and 110%. Primer sequences and information can be found in Table S2.

All qPCRs were performed in 20-µL mixtures containing 10 µL of SYBR Green Master Mix (2×) (Thermo Fisher Scientific, Cat. No. A25742), 0.5 µM of each primer, 2 µL of DNA template, and nuclease-free water to meet the volume. qPCRs were performed in 384-Well Clear Reaction plates (Applied Biosystems, Cat. No. 4483285) (for qPCRs), loaded to a QuantStudio 5 Real-Time PCR system (Applied Biosystems), and were run under the following conditions: pre-incubation at 50°C for 2 min, polymerase activation at 95°C for 10 s, followed by 40 cycles, each at 95°C for 15 s, 55°C for 15 s, and 72°C for 1 min. Amplification specificity was confirmed by melt curve analysis under the following conditions: 95°C for 15 s; 60°C for 1 min, and 95°C for 15 s. qPCR reactions were performed in technical triplicates with a non-template control, RNA extraction control, and a no reverse transcriptase control (−RT). Two nanograms of cDNA was used for qPCR, and the relative expression was calculated by the $2^{-\Delta\Delta CT}$ method.

RNAseq was performed by Eurofins Genomics (Germany) using Illumina NovaSeq. Raw sequencing data were pre-processed to generate high-quality data for downstream analyses. Reads originating from ribosomal RNA (rRNA) were identified and removed using RiboDetector (35). The remaining non-rRNA reads were subjected to quality control using fastp (36), including adapter trimming, removal of low-quality bases (Phred quality score <20), and per-read quality pruning using a sliding-window approach. After quality trimming, reads shorter than 30 bp were discarded. For paired-end sequencing, only read pairs in which both reads passed quality control were retained. Sequencing quality was assessed using standard metrics, including the proportion of bases with Phred quality score ≥30 (Q30) and GC content (Table S3). High-quality reads were aligned to the *B. infantis* DSM 20088 reference genome using STAR (Spliced Transcripts Alignment to a Reference) (37) within the Sentieon framework (38), incorporating known gene models. STAR was used to perform spliced read alignment optimized for RNA-seq data. Gene-level quantification was performed using featureCounts (39). Low-expressed genes were filtered prior to downstream analyses by removing genes with counts per million values <1. The abundance counts of each gene were then used to perform differential gene expression (DGE). DGE was performed using the edgeR package (40) from Bioconductor. Library sizes were normalized using the calcNormFactors() function to correct for differences in RNA composition between samples. Statistical comparisons between experimental conditions were performed for each gene, and *P* values were adjusted for multiple testing using the Benjamini–Hochberg false discovery rate (FDR) method. Genes with average read counts greater than 100 across all samples, and FDR-adjusted *P* values < 0.1 were considered differentially expressed.

Statistics

All statistical analyses, except for DGE, were carried out in GraphPad Prism software (v. 10.4.1). For the AAA availability test, statistical significance between groups was

determined by one-way analysis of variance (ANOVA), followed by Tukey's multiple comparisons test. For the chemostat experiments, cell densities were compared using repeated measures two-way ANOVA, followed by Bonferroni correction for multiple comparisons test. Metabolite differences in the chemostat experiments were compared using two-way ANOVA. Relative percent-wise abundance of ALAs was assessed by the chi-square test. Relative *aldh* expression between groups was compared using an unpaired two-tailed *t*-test with Welch's correction on gene expression values normalized to reference genes at each time point. All correlations were Pearson correlations. For all statistical analyses, if not stated otherwise, a P value < 0.05 was considered significant.

ACKNOWLEDGMENTS

We thank Anurag Kumar Sinha, Julius Emil Brinck, and Emmelie Joe Freudenberg Rasmussen (National Food Institute, Technical University of Denmark) for technical advice concerning chemostat fermentations. Moreover, we thank Bodil Madsen and Katja Ann Kristensen (National Food Institute, Technical University of Denmark) for technical support in the laboratory.

This study was funded by a grant from the Novo Nordisk Foundation Challenge program (PRIMA, grant number NNF19OC0056246).

AUTHOR AFFILIATION

[1]National Food Institute, Technical University of Denmark, Kongens Lyngby, Denmark

AUTHOR ORCIDs

Thilde Garbøl Plenge http://orcid.org/0009-0004-8761-3690
Mikael Pedersen https://orcid.org/0000-0001-6540-4805
Martin Frederik Laursen http://orcid.org/0000-0001-6017-7121

FUNDING

Funder	Grant(s)	Author(s)
Novo Nordisk Fonden	NNF19OC0056246	Martin Frederik Laursen

AUTHOR CONTRIBUTIONS

Thilde Garbøl Plenge, Conceptualization, Data curation, Formal analysis, Investigation, Methodology, Visualization, Writing – original draft | Mikael Pedersen, Data curation, Formal analysis, Methodology, Resources | Martin Frederik Laursen, Conceptualization, Data curation, Formal analysis, Funding acquisition, Investigation, Methodology, Project administration, Supervision, Validation, Visualization, Writing – review and editing

DATA AVAILABILITY

Raw sequencing data have been deposited in the European Nucleotide Archive (ENA) under accession number PRJEB105461.

ADDITIONAL FILES

The following material is available online.

Supplemental Material

Supplemental material (AEM02511-25-s0001.docx). Fig. S1 to S5; Tables S1 to S4.

REFERENCES

1. Bode L. 2012. Human milk oligosaccharides: every baby needs a sugar mama. Glycobiology 22:1147–1162. https://doi.org/10.1093/glycob/cws074
2. Ward RE, Niñonuevo M, Mills DA, Lebrilla CB, German JB. 2007. *In vitro* fermentability of human milk oligosaccharides by several strains of bifidobacteria. Mol Nutr Food Res 51:1398–1405. https://doi.org/10.1002/mnfr.200700150
3. Laursen MF, Roager HM. 2023. Human milk oligosaccharides modify the strength of priority effects in the *Bifidobacterium* community assembly during infancy. ISME J 17:2452–2457. https://doi.org/10.1038/s41396-023-01525-7
4. Underwood MA, German JB, Lebrilla CB, Mills DA. 2015. *Bifidobacterium longum* subspecies *infantis*: champion colonizer of the infant gut. Pediatr Res 77:229–235. https://doi.org/10.1038/pr.2014.156
5. Laursen MF, Sakanaka M, von Burg N, Mörbe U, Andersen D, Moll JM, Pekmez CT, Rivollier A, Michaelsen KF, Mølgaard C, Lind MV, Dragsted LO, Katayama T, Frandsen HL, Vinggaard AM, Bahl MI, Brix S, Agace W, Licht TR, Roager HM. 2021. Bifidobacterium species associated with breastfeeding produce aromatic lactic acids in the infant gut. Nat Microbiol 6:1367–1382. https://doi.org/10.1038/s41564-021-00970-4
6. Zelante T, Iannitti RG, Cunha C, De Luca A, Giovannini G, Pieraccini G, Zecchi R, D'Angelo C, Massi-Benedetti C, Fallarino F, Carvalho A, Puccetti P, Romani L. 2013. Tryptophan catabolites from microbiota engage aryl hydrocarbon receptor and balance mucosal reactivity via interleukin-22. Immunity 39:372–385. https://doi.org/10.1016/j.immuni.2013.08.003
7. Natividad JM, Agus A, Planchais J, Lamas B, Jarry AC, Martin R, Michel M-L, Chong-Nguyen C, Roussel R, Straube M, et al. 2018. Impaired aryl hydrocarbon receptor ligand production by the gut microbiota is a key factor in metabolic syndrome. Cell Metab 28:737–749. https://doi.org/10.1016/j.cmet.2018.07.001
8. Peters A, Krumbholz P, Jäger E, Heintz-Buschart A, Çakir MV, Rothemund S, Gaudl A, Ceglarek U, Schöneberg T, Stäubert C. 2019. Metabolites of lactic acid bacteria present in fermented foods are highly potent agonists of human hydroxycarboxylic acid receptor 3. PLoS Genet 15:e1008145. https://doi.org/10.1371/journal.pgen.1008145
9. Sakurai T, Horigome A, Odamaki T, Shimizu T, Xiao JZ. 2021. Production of hydroxycarboxylic acid receptor 3 (Hca3) ligands by *Bifidobacterium*. Microorganisms 9:2397. https://doi.org/10.3390/microorganisms9112397
10. Lavermicocca P, Valerio F, Visconti A. 2003. Antifungal activity of phenyllactic acid against molds isolated from bakery products. Appl Environ Microbiol 69:634–640. https://doi.org/10.1128/AEM.69.1.634-640.2003
11. Ning Y, Yan A, Yang K, Wang Z, Li X, Jia Y. 2017. Antibacterial activity of phenyllactic acid against *Listeria monocytogenes* and *Escherichia coli* by dual mechanisms. Food Chem 228:533–540. https://doi.org/10.1016/j.foodchem.2017.01.112
12. Guimarães A, Santiago A, Teixeira JA, Venâncio A, Abrunhosa L. 2018. Anti-aflatoxigenic effect of organic acids produced by *Lactobacillus plantarum*. Int J Food Microbiol 264:31–38. https://doi.org/10.1016/j.ijfoodmicro.2017.10.025
13. Chatzigiannidou I, Johansen PL, Dehli RK, Moll JM, Eriksen C, Myers PN, Roager HM, Yang L, Stokholm J, Sørensen SJ, Krogfelt KA, Laursen MF, Trivedi U, Scheynius A, Kristiansen K, Mie A, Alm J, Brix S. 2025. Temporal dynamics and microbial interactions shaping the gut resistome in early infancy. Nat Commun 16:8139. https://doi.org/10.1038/s41467-025-63401-6
14. Myers PN, Dehli RK, Mie A, Moll JM, Roager HM, Eriksen C, Laursen MF, Staudinger EM, Chatzigiannidou I, Johansen PL, et al. 2026. Early-life colonization by aromatic-lactate-producing bifidobacteria lowers the risk of allergic sensitization. Nat Microbiol 11:429–441. https://doi.org/10.1038/s41564-025-02244-9
15. Roager HM, Hansen LBS, Bahl MI, Frandsen HL, Carvalho V, Gøbel RJ, Dalgaard MD, Plichta DR, Sparholt MH, Vestergaard H, Hansen T, Sicheritz-Pontén T, Nielsen HB, Pedersen O, Lauritzen L, Kristensen M, Gupta R, Licht TR. 2016. Colonic transit time is related to bacterial metabolism and mucosal turnover in the gut. Nat Microbiol 1:16093. https://doi.org/10.1038/nmicrobiol.2016.93
16. Lewis SJ, Heaton KW. 1997. Increasing butyrate concentration in the distal colon by accelerating intestinal transit. Gut 41:245–251. https://doi.org/10.1136/gut.41.2.245
17. Ma J, Li Z, Zhang W, Zhang C, Zhang Y, Mei H, Zhuo N, Wang H, Wang L, Wu D. 2020. Comparison of gut microbiota in exclusively breast-fed and formula-fed babies: a study of 91 term infants. Sci Rep 10. https://doi.org/10.1038/s41598-020-72635-x
18. Purkiewicz A, Stasiewicz M, Nowakowski JJ, Pietrzak-Fiećko R. 2023. The influence of the lactation period and the type of milk on the content of amino acids and minerals in human milk and infant formulas. Foods 12:3674. https://doi.org/10.3390/foods12193674
19. Mu W, Yu S, Zhu L, Jiang B, Zhang T. 2012. Production of 3-phenyllactic acid and 4-hydroxyphenyllactic acid by *Pediococcus acidilactici* DSM 20284 fermentation. Eur Food Res Technol 235:581–585. https://doi.org/10.1007/s00217-012-1768-x
20. Henrick BM, Hutton AA, Palumbo MC, Casaburi G, Mitchell RD, Underwood MA, Smilowitz JT, Frese SA. 2018. Elevated fecal pH indicates a profound change in the breastfed infant gut microbiome due to reduction of *Bifidobacterium* over the past century. mSphere 3:e00041-18. https://doi.org/10.1128/mSphere.00041-18
21. Wei Y, Gao J, Liu D, Li Y, Liu W. 2019. Adaptational changes in physiological and transcriptional responses of *Bifidobacterium longum* involved in acid stress resistance after successive batch cultures. Microb Cell Fact 18:156. https://doi.org/10.1186/s12934-019-1206-x
22. Schöpping M, Zeidan AA, Franzén CJ. 2022. Stress response in bifidobacteria. Microbiol Mol Biol Rev 86:e0017021. https://doi.org/10.1128/mmbr.00170-21
23. Shiver AL, Sun J, Culver R, Violette A, Wynter C, Nieckarz M, Mattiello SP, Sekhon PK, Bottacini F, Friess L, et al. 2025. Genome-scale resources in the infant gut symbiont *Bifidobacterium breve* reveal genetic determinants of colonization and host-microbe interactions. Cell 188:2003–2021. https://doi.org/10.1016/j.cell.2025.02.010
24. Valerio F, Lavermicocca P, Pascale M, Visconti A. 2004. Production of phenyllactic acid by lactic acid bacteria: an approach to the selection of strains contributing to food quality and preservation. FEMS Microbiol Lett 233:289–295. https://doi.org/10.1016/j.femsle.2004.02.020
25. Sinha AK, Laursen MF, Brinck JE, Rybtke ML, Hjørne AP, Procházková N, Pedersen M, Roager HM, Licht TR. 2024. Dietary fibre directs microbial tryptophan metabolism via metabolic interactions in the gut microbiota. Nat Microbiol 9:1964–1978. https://doi.org/10.1038/s41564-024-01737-3
26. Li X, Jiang B, Pan B. 2007. Biotransformation of phenylpyruvic acid to phenyllactic acid by growing and resting cells of a *Lactobacillus* sp. Biotechnol Lett 29:593–597. https://doi.org/10.1007/s10529-006-9275-4
27. Mu W, Liu F, Jia J, Chen C, Zhang T, Jiang B. 2009. 3-phenyllactic acid production by substrate feeding and pH-control in fed-batch fermentation of *Lactobacillus* sp. SK007. Bioresour Technol 100:5226–5229. https://doi.org/10.1016/j.biortech.2009.05.024
28. Laursen MF, Sinha AK, Pedersen M, Roager HM. 2023. Key bacterial taxa determine longitudinal dynamics of aromatic amino acid catabolism in infants' gut. Gut Microbes 15:2221426. https://doi.org/10.1080/19490976.2023.2221426
29. Sánchez B, Champomier-Vergès M-C, Collado M del C, Anglade P, Baraige F, Sanz Y, de los Reyes-Gavilán CG, Margolles A, Zagorec M. 2007. Low-pH adaptation and the acid tolerance response of *Bifidobacterium longum* biotype *longum*. Appl Environ Microbiol 73:6450–6459. https://doi.org/10.1128/AEM.00886-07
30. Frese SA, Hutton AA, Contreras LN, Shaw CA, Palumbo MC, Casaburi G, Xu G, Davis JCC, Lebrilla CB, Henrick BM, Freeman SL, Barile D, German JB, Mills DA, Smilowitz JT, Underwood MA. 2017. Persistence of supplemented *Bifidobacterium longum* subsp. *infantis* EVC001 in breastfed infants. mSphere 2. https://doi.org/10.1128/mSphere.00501-17
31. Vermeulen N, Ganzle MG, Vogel RF. 2006. Influence of peptide supply and cosubstrates on phenylalanine metabolism of *Lactobacillus sanfranciscensis* DSM20451^T and *Lactobacillus plantarum* TMW1.468. J Agric Food Chem 54:3832–3839. https://doi.org/10.1021/jf052733e
32. Kasperek MC, Velasquez Galeas A, Caetano-Silva ME, Xie Z, Ulanov A, La Frano M, Devkota S, Miller MJ, Allen JM. 2024. Microbial aromatic amino acid metabolism is modifiable in fermented food matrices to promote bioactivity. Food Chem 454:139798. https://doi.org/10.1016/j.foodchem.2024.139798
33. De MAN JC, Rogosa M, Sharpe ME. 1960. A medium for the cultivation of lactobacilli. J Appl Bacteriol 23:130–135. https://doi.org/10.1111/j.1365-2672.1960.tb00188.x

34. Turroni F, Foroni E, Montanini B, Viappiani A, Strati F, Duranti S, Ferrarini A, Delledonne M, van Sinderen D, Ventura M. 2011. Global genome transcription profiling of *Bifidobacterium bifidum* PRL2010 under *in vitro* conditions and identification of reference genes for quantitative real-time PCR. Appl Environ Microbiol 77:8578–8587. https://doi.org/10.1128/AEM.06352-11
35. Deng ZL, Münch PC, Mreches R, McHardy AC. 2022. Rapid and accurate identification of ribosomal RNA sequences via deep learning. Nucleic Acids Res 50:e60. https://doi.org/10.1093/nar/gkac112
36. Chen S, Zhou Y, Chen Y, Gu J. 2018. fastp: an ultra-fast all-in-one FASTQ preprocessor. Bioinformatics 34:i884–i890. https://doi.org/10.1093/bioinformatics/bty560
37. Dobin A, Davis CA, Schlesinger F, Drenkow J, Zaleski C, Jha S, Batut P, Chaisson M, Gingeras TR. 2013. STAR: ultrafast universal RNA-seq aligner. Bioinformatics 29:15–21. https://doi.org/10.1093/bioinformatics/bts635
38. Sentieon. 2011. Sentieon provides complete solutions for secondary dna/rna analysis for a variety of sequencing platforms, including short and long reads. Available from: https://www.sentieon.com
39. Liao Y, Smyth GK, Shi W. 2014. featureCounts: an efficient general purpose program for assigning sequence reads to genomic features. Bioinformatics 30:923–930. https://doi.org/10.1093/bioinformatics/btt656
40. Robinson MD, McCarthy DJ, Smyth GK. 2010. edgeR: a bioconductor package for differential expression analysis of digital gene expression data. Bioinformatics 26:139–140. https://doi.org/10.1093/bioinformatics/btp616